Available online at www.sciencedirect.com
ScienceDirect
Phytochemistry 68 (2007) 2232–2242
PHYTOCHEMISTRY
www.elsevier.com/locate/phytochem

Parallel determination of enzyme activities and *in vivo* fluxes in *Brassica napus* embryos grown on organic or inorganic nitrogen source

Björn H. Junker [a], Joachim Lonien [a], Lindsey E. Heady [b], Alistair Rogers [b,c], Jörg Schwender [a,*]

[a] *Biology Department, Brookhaven National Laboratory, Upton, NY 11973, United States*
[b] *Environmental Sciences Department, Brookhaven National Laboratory, Upton, NY 11973, United States*
[c] *Department of Crop Sciences, University of Illinois, Urbana, IL 61801, United States*

Received 23 January 2007; received in revised form 22 March 2007
Available online 16 May 2007

Abstract

After the completion of the genomic sequencing of model organisms, numerous post-genomic studies, integrating transcriptome and metabolome data, are aimed at developing a more complete understanding of cell physiology. Here, we measure *in vivo* metabolic fluxes by steady state labeling, and in parallel, the activity of enzymes in central metabolism in cultured developing embryos of *Brassica napus*. Embryos were grown on either the amino acids glutamine and alanine as an organic nitrogen source, or on ammonium nitrate as an inorganic nitrogen source. The type of nitrogen made available to developing embryos caused substantial differences in fluxes associated with the tricarboxylic acid cycle, including flux reversion. The changes observed in enzyme activity were not consistent with our estimates of metabolic flux. Furthermore, most extractable enzyme activities are in large surplus relative to the requirements for the observed *in vivo* fluxes. The results demonstrate that in this model system the metabolic response of central metabolism to changes in environmental conditions can be achieved largely without regulatory reprogramming of the enzyme machinery.

Keywords: *Brassica napus*; Central metabolism; Enzyme activity profiling; Metabolic flux analysis

1. Introduction

Current approaches in plant systems biology are aiming at comprehensively describing the living cell at several organizational levels: genes (The Arabidopsis Genome Initiative, 2000), transcripts (Ruuska et al., 2002), and metabolites (Roessner et al., 2001). Major goals of these approaches are the functional identification of unknown genes as well as the integrated understanding of gene regulation and metabolism. More recently, approaches to acquire and compare data in parallel from the different organizational levels are gaining interest. Transcripts and metabolites have been analyzed in parallel in plants and numerous significant and biologically relevant correlations between transcripts and metabolites have been found (Urbanczyk-Wochniak et al., 2003; Hirai et al., 2004; Scheible et al., 2004; Hirai et al., 2005; Tohge et al., 2005). Also, transcript levels and enzyme activities have been correlated in *Arabidopsis thaliana* (Gibon et al., 2004; Morcuende et al., 2007) and in *Brassica napus* developing seeds (Li et al., 2006).

The functional relation between an enzyme and its respective substrates are biochemically very exactly defined through stoichiometry and kinetic rate laws. However, to our knowledge, there have been no studies comparing enzyme activities and steady state metabolic flux analysis in plants, and only few such studies in microbial systems (Petersen et al., 2001). However, doing this has an appealing motivation: in theory, enzyme levels and *in vivo* conversion rates (fluxes) should correlate, making flux predictable. At least it can be stated that extractable enzyme

* Corresponding author. Tel.: +1 631 344 3797; fax: +1 631 344 3407.
E-mail address: schwender@bnl.gov (J. Schwender).

0031-9422/$ - see front matter © 2007 Elsevier Ltd. All rights reserved.
doi:10.1016/j.phytochem.2007.03.032

activity, measured under substrate saturation, is a good measure for maximal possible *in vivo* flux. Related to this it had been frequently assumed that certain enzymes in pathways are rate limiting, an idea that has been mostly abandoned in the light of results from metabolic control theory (Kacser and Burns, 1973; Heinrich and Rapoport, 1974; Fell, 1997).

In this paper, we compare metabolic fluxes and enzyme activities measured in parallel in cultures of developing embryos of *Brassica napus* (cv. Reston) grown under two different nutritional conditions. *In planta* rapeseed embryos derive their nitrogen from amino acids transported from the parental seed coat (Schwender and Ohlrogge, 2002) and in culture they can be grown with the amino acids Ala and Gln as the sole nitrogen source (Schwender et al., 2006). However, they can also be grown with inorganic ammonium nitrate instead (Schwender and Ohlrogge, 2002). Since the formation of storage proteins is a major metabolic activity in developing *B. napus* embryos a change in nitrogen source should entail major adjustments in C/N metabolism, affecting reactions related to amino acid metabolism and the tricarboxylic acid (TCA) cycle. While Gln and Ala deliver nitrogen in an already reduced form and bound to an organic acid which can be used in intermediary metabolism, embryos growing on NH_4NO_3 have to reduce the nitrogen by pathways of primary nitrogen assimilation. Based on former metabolic flux analysis and biochemical studies in developing *B. napus* embryos (Schwender and Ohlrogge, 2002; Schwender et al., 2003, 2004, 2006; Goffman et al., 2005; Ruuska et al., 2004) we investigated potential adjustments in C/N metabolism by comparing developing *B. napus* embryos cultured using media with two different nitrogen sources: (1) an organic nitrogen source, the amino acids Gln and Ala and (2) an inorganic nitrogen source, NH_4NO_3. We measured 16 steady state metabolic fluxes in central metabolism and the activities of 22 enzymes. The results shed light on the flexibility of metabolism in response to change in nutritional conditions and show that such metabolic adjustment is probably not mediated by changes in enzyme levels.

2. Results and discussion

2.1. Culture system

B. napus (cv. Reston) developing embryos were grown for 12 days in aseptic culture under continuous low light as described in Section 4. Two different exclusive nitrogen sources were provided: either the amino acids Gln and Ala (Schwender et al., 2003, 2006), which mimics the *in planta* nutritional situation, or the inorganic nitrogen source ammonium nitrate (Schwender and Ohlrogge, 2002). Preconditions for the interpretation of the results are that (1) with respect to flux analysis both metabolic and isotopic steady state are given during the 12 days growth period and (2) the enzyme activities measured after 12 days culture still represent the same metabolic steady state. As previously established for the model system used in this study (Schwender et al., 2006), the culture conditions maintained (in approximation) a steady state over the period of measurement under both conditions, embryo fresh weight (fw) continuously increased approximating a logistic growth curve with biomass increase per g fw almost constant. The same growth characteristics continued after the 12 day sampling stage, indicating that at the time of harvest the embryos were in a steady metabolic active state and were still accumulating storage compounds. Despite the similar growth characteristics, for the inorganic N source only about 50% the growth rate was achieved as compared to the amino acid medium. This may indicate that the use of inorganic nitrogen limits growth to a certain extent, possibly since substantial amounts of reducing equivalents are needed for the assimilation of ammonia and/or nitrate. In addition, between the two growth conditions a difference in biomass composition was observed (Table 1). When embryos were grown with an organic N supply the lipid and protein content were close to the previously observed values (Schwender et al., 2006), when grown with an inorganic N supply, the lipid content was 4.5% higher and the protein content was 4.6% lower (Table 1). The difference in biomass composition was considered for flux analysis (see Section 4) resulting in increased flux towards lipid synthesis and decreased fluxes towards amino acids used for storage protein synthesis. However, the changes in flux distribution due to change of N-nutrition are much more pronounced and are the focus of this paper.

2.2. Flux analysis

For growth on the inorganic nitrogen source, embryos were labeled in separate experiments with [1-^{13}C]glucose and [U-$^{13}C_6$]glucose (Table 2). Flux parameter fitting

Table 1
Biomass parameters for *B. napus* embryos grown for 12 days with two different nitrogen sources

	Nitrogen source	
	Organic (Gln/Ala)	Inorganic (NH_4NO_3)
Fw/embryo [mg]	21.3 ± 6.8	9.3 ± 1.8
Lipids [% wt/dw]	38.1 ± 1.0	42.6 ± 1.1
Protein [% wt/dw]	17.9 ± 0.3	13.3 ± 0.9
Cell pellet–protein [% wt/dw]	24.6 ± 1.2	31.9 ± 1.1
Methanol/H_20 fraction [% wt/dw]	19.5 ± 0.4	12.1 ± 0.7

Analysis of embryo tissue as described in Section 4. Average ± SE ($n = 3$) given for fresh weight (fw) and dry weight (dw) fractions. Water content was 52.6 ± 0.8% and 51.3 ± 0.4% for growth on Gln/Ala and NH_4NO_3, respectively. The methanol/water fraction contains sugars (sucrose, glucose, fructose) and amino acids as major components (as determined by gas chromatography–mass spectrometry after trimethyl-silyl derivatization, data not shown).

Table 2
Labeling in amino acids, fatty acids and starch (glucose) after growth in NH_4NO_3-medium with [1-^{13}C]glucose or [U-$^{13}C_6$]glucose

Fragment (carbon atoms)	Mass isotopomer	[1-^{13}C]glucose		[U-$^{13}C_6$]glucose	
		Measured% (SD%)	Predicted%	Measured% (SD%)	Predicted%
Ala 260(1–3)	m_0	86.15 (0.79)	86.58	47.27 (0.19)	46.99
	m_1	13.49 (0.79)	11.34	12.14 (0.25)	12.85
	m_2	0.36 (0.03)	0.29	11.67 (0.07)	11.83
	m_3	−0.01 (0.02)	0.00	28.92 (0.13)	28.84
Ala 232(2–3)	m_0	87.13 (0.78)	87.44	55.61 (0.09)	55.65
	m_1	12.80 (0.77)	10.17	6.51 (0.19)	6.52
	m_2	0.06 (0.01)	0.00	37.88 (0.27)	37.35
C18 74(1–2)	m_0	86.81 (0.70)	87.16		0
	m_1	13.27 (0.70)	10.14		0
	m_2	−0.07 (3E−3)	0.00		0
C22 74(1–2)	m_0	87.84 (0.56)	87.87		0
	m_1	12.23 (0.56)	10.22		0
	m_2	−0.07 (0.00)	0.00		0
C22(1)[a]	m_0	99.06 (0.07)	99.06		0
	m_1	0.85 (0.08)	0.72		0
Pro 286(1–5)	m_0	74.07 (0.75)	74.75	22.51 (1.71)	21.95
	m_1	23.58 (0.88)	20.94	15.23 (0.35)	14.41
	m_2	2.46 (0.24)	1.89	25.87 (0.98)	27.11
	m_3	−0.07 (0.34)	0.05	19.77 (0.57)	21.05
	m_4	−0.03 (0.02)	0.00	8.93 (0.13)	8.77
	m_5	−0.01 (0.02)	0.00	7.69 (0.16)	7.93
Pro 184(2–5)	m_0	76.23 (0.79)	77.77	31.75 (1.20)	32.26
	m_1	22.10 (0.67)	18.09	9.56 (0.26)	7.60
	m_2	1.51 (0.13)	1.05	39.06 (1.52)	43.73
	m_3	0.11 (0.01)	0.00	5.95 (0.18)	5.10
	m_4	0.05 (1E−3)	0.00	13.68 (0.22)	14.53
Asp 418(1–4)	m_0	82.66 (0.85)	81.98	27.74 (1.31)	27.75
	m_1	16.66 (0.74)	17.39	24.77 (1.03)	28.47
	m_2	0.66 (0.11)	1.16	15.15 (0.04)	15.13
	m_3	0.00 (0.04)	0.02	20.55 (0.71)	22.48
	m_4	0.02 (2E−3)	0.00	11.80 (0.42)	11.40
Asp 316(2–4)	m_0	83.93 (0.62)	84.07	37.37 (0.89)	38.54
	m_1	14.87 (0.58)	13.77	21.29 (0.47)	20.77
	m_2	0.50 (0.03)	0.52	20.73 (0.53)	19.30
	m_3	0.71 (0.03)	0.00	20.61 (0.18)	20.76
Asp 302(1–2)	m_0	91.99 (0.30)	91.82	42.93 (1.04)	44.62
	m_1	7.85 (0.31)	9.24	31.50 (1.25)	40.39
	m_2	0.16 (0.04)	0.35	25.57 (0.30)	24.48
PP(1–5)[b]	m_0	73.54 (1.46)	73.38		
	m_1	23.34 (1.09)	24.50		
	m_2	2.84 (0.28)	2.20		
	m_3	0.19 (0.08)	0.05		
	m_4	0.11 (0.04)	0.00		
	m_5	−0.01 (0.01)	0.00		
Glucose 360(1–6)	m_0	78.43 (0.98)	76.90		
	m_1	19.67 (0.73)	22.78		
	m_2	1.64 (0.26)	0.87		
	m_3	0.27 (0.07)	0.03		
	m_4	0.01 (0.03)	0.00		
	m_5	−0.02 (2E−3)	0.00		
	m_6	0.00 (3E−4)	0.00		
Glucose 89(1–2)	m_0	83.57 (0.91)	82.68		
	m_1	16.26 (0.92)	19.98		
	m_2	0.17 (0.01)	0.00		

(*continued on next page*)

Table 2 (*continued*)

Fragment (carbon atoms)	Mass isotopomer	[1-^{13}C]glucose		[U-$^{13}C_6$]glucose	
		Measured% (SD%)	Predicted%	Measured% (SD%)	Predicted%
Glucose 289(2–6)	m_0	93.72 (0.46)	93.81		
	m_1	4.94 (0.35)	1.19		
	m_2	0.30 (0.05)	0.01		
	m_3	0.51 (0.05)	0.00		
	m_4	0.52 (0.04)	0.00		

Measured and model predicted steady state mass isotopomer fractions, after derivatization and analysis by GC–MS as described in Section 4. SD for $n = 3$ biological repetitions. Fragments are given with molecular weight and the carbons of the metabolite which are included in the fragment. Model predicted values are the best fit corresponding to the flux values in Table 3.

[a] Fragment *m/z* 74 (carbons one and two) of C22 (Docosanoioc acid methyl ester), together with the fragment *m/z* 87 (carbons one, two and three; Murphy, 1993) allows to calculate the ^{13}C-enrichment in carbon one by probabilistic equations assuming that odd-numbered carbons are derived from carbon one of acetyl-CoA.

[b] The labeling in pentose phosphate (PP) was derived from $His_{(1-6)}$ by considering the label in the ε-carbon of His (derived from C-1 metabolism) to be equal to Gly(2) as described earlier (Schwender et al., 2006).

resulted in flux values (Table 3) which best explain the labeling data obtained from using both [1-^{13}C]glucose and [U-$^{13}C_6$]glucose. The flux distribution for growth on the organic nitrogen source (Table 3) was taken from a previous study (Schwender et al., 2006), where *B. napus* cv. Reston embryos were grown under identical conditions as used for this experiment. A flux map of central metabolism had been established using computer assisted ^{13}C-flux steady state flux analysis with multiple different ^{13}C- and ^{15}N-labeled tracers (Schwender et al., 2006). In particular, the use of ^{13}C-labeled Ala and Gln allowed the resolution of fluxes between sub-cellular compartments and enabled us to obtain more reliable flux estimates than those possible using only ^{13}C-glucose (Schwender et al., 2006). In this study, under the inorganic nitrogen condition, we could use only glucose tracers ([1-^{13}C]glucose, [U-$^{13}C_6$]glucose) due to the absence of amino acids from the growth medium. However, based on details on network topology that were established in the former study, reliable flux analysis was still possible (see Section 4.3).

2.3. Flux distribution

Between the two nutritional conditions we observed a profound shift in fluxes associated with the TCA cycle. In Table 3 and Fig. 2 a comparison of fluxes for essential reactions associated with the TCA cycle is shown. Comparison of metabolic fluxes in central metabolism between different conditions is usually done based on normalization of fluxes, like scaling fluxes relative to the substrate uptake flux set to 100% (see e.g. Rontein et al., 2002; Yang et al., 2002a). While the measured ^{13}C-labeling signatures (Table 2) essentially define fluxes relative to each other, we define absolute flux values indirectly by growth rate measurements (Schwender et al., 2006). Under the NH_4NO_3 condition we observed only about 50% of the growth rate we measured for the Gln/Ala condition, resulting in significant differences in almost all fluxes (data not shown). In order to allow a more meaningful comparison of the flux rates, the fluxes of the NH_4NO_3 condition shown in Table 3 are scaled according to the same growth rate as observed under the Gln/Ala condition. This resulted in similar fluxes into biomass (amino acids, lipids) under both conditions (Table 3). The conclusions we draw based on this normalization are the same as if the comparison is made by normalizing substrate uptake (data not shown).

As shown in Fig. 2, the major metabolic flux is going through glycolysis and is directed via pyruvate towards fatty acid synthesis. The glycolytic flux (pyruvate kinase, PK, EC 2.7.1.40) is 26% larger in embryos growing with an inorganic N supply (Table 3). This can be explained by the fact that embryos grown with an organic N source will have a lower demand for carbon skeletons to build amino acids for protein synthesis (Schwender and Ohlrogge, 2002) whereas embryos developing with an inorganic N supply must derive their carbon skeletons from glycolytic intermediates.

The main difference between the organic and the inorganic nitrogen condition is characterized by redirection of fluxes leading into and out of the TCA cycle (Table 3, Fig. 2). Under the organic nitrogen condition, about 30% of the absorbed Gln enters the TCA cycle after being transformed to α-ketoglutarate (KG) (Fig. 2A). Under the inorganic nitrogen condition Gln is not available, and therefore KG has to be withdrawn from the TCA cycle to supply Gln, Glu, Pro and Arg for protein synthesis (Fig. 2B). Consequently, the depleted TCA cycle intermediates have to be refilled by anaplerotic reactions. As illustrated by Fig. 2, this adjustment appears to be made by significant reduction in mitochondrial NAD-malic enzyme (NAD-ME, EC 1.1.1.39) flux as well as by significant increase in phosphoenol pyruvate carboxylase (PEPC, EC 4.1.1.3) flux (Table 2).

Notably, cyclic flux through the TCA cycle is absent with the organic nitrogen source (isocitrate dehydrogenase with only negligible net flux; Table 3) and minor with the inorganic nitrogen source (Fumarase net flux small relative to other TCA cycle fluxes). This again suggests that in developing oilseeds, the cyclic oxidation of pyruvate by the TCA cycle plays only a minor role in metabolism as compared to the metabolic interconversion of TCA cycle intermediates for biosynthetic purposes. A consequence

Table 3
Values for net fluxes (±95% confidence interval of the mean) derived by flux parameter fitting (nmol min^{-1} g fw^{-1})

Enzymes	Reaction	Nutritional condition	
		Organic Gln/Ala	Inorganic NH_4NO_3
Sugar uptake (sucrose, glucose, and hexose units)		972.1 ± 79.4	1268.7 ± 94.4*
Ala uptake	→ Ala	122.8 ± 13.5	0*
Gln uptake	→ Gln	70.9 ± 5.8	0*
Alanine:KG aminotransferase	Ala → Pyr	110.8 ± 13.5	−9.4 ± 1.9*
Pyruvate kinase	PEP → Pyr	1297.8 ± 160.1	1636.0 ± 183.1
Phosphoenol pyruvate carboxylase**	PEP → OAA	59.4 ± 6.2	91.2 ± 9.9*
Pyruvate dehydrogenase, **Citrate synthase**	OAA + Pyr → Citrate + CO_2	97.0 ± 11.4	148.8 ± 15.6*
Mitochondrial malic enzyme	Malate → Pyr + CO_2	39.0 ± 6.5	19.8 ± 2.7*
Aconitase, **Isocitrate dehydrogenase**	Citrate → Isocitrate → KG	−1.3 ± 3.3	50.4 ± 6.6*
Ketoglutarate dehydrogenase, Succinyl-CoA synthetase, Succinate dehydrogenase, **Fumarase**	KG → malate	22.0 ± 3.9	13.2 ± 1.7*
ATP:citrate lyase	Citrate → OAA + acetyl-CoA	98.3 ± 12.1	98.3 ± 13.9
Glutamate synthase	Gln → Glu	49.7 ± 4.7	−16.6 ± 3.6*
Transaminases, **Glutamate dehydrogenase**, dicarboxylate transporter	Glu → KG	23.4 ± 3.2	−37.2 ± 5.5*
Alanine into protein	Ala → Ala_p	12.0 ± 1.9	9.4 ± 1.9
Aspartate into protein	Asp → Asp_p	43.8 ± 6.4	34.2 ± 6.9
Glutamate into protein	Glu → Glu_p	26.3 ± 4.2	20.6 ± 4.2
Glutamine into protein	Gln → Gln_p	21.2 ± 3.6	16.6 ± 3.6
Pyruvate dehydrogenase, fatty acid synthesis, Lipid assembly	Pyr → TAG	1366.3 ± 167.9	1531.6 ± 168.3

The flux values for the Gln/Ala nutritional condition are taken from Schwender et al. (2006) and scaled to the unit presented in this table. The flux values for the NH_4NO_3 condition result from analysis of labeling with [1-^{13}C]glucose ($n = 3$) and [U-$^{13}C_6$]glucose ($n = 3$) in this study. For comparison the flux values of the NH_4NO_3 condition are scaled according to the same growth rate (biomass flux) as for the Gln/Ala condition (Schwender et al., 2006). Significant changes in fux ($p = 0.05$) are indicated by asterisk. Enzymes for which the activities have been measured in this study are formatted bold, with significant changes denoted by a double asterisk (see Fig. 1). For abbreviations see the legend of Fig. 2.

of the low cyclic flux is low contribution via oxidative phosphorylation to the total ATP balance of the embryo. This has been described before for the organic nitrogen growth condition (Schwender et al., 2006) and seems also to apply for the inorganic nitrogen condition as well.

2.4. Enzyme activities

The maximal catalytic activities of 22 enzymes of central metabolism were measured under substrate saturation using a recently developed platform (Gibon et al., 2004). The resulting enzyme activities are shown in Fig. 1. The activities of different enzymes span several orders of magnitude ranging from relatively low activity of glycerokinase (GlyK, EC 2.7.1.30) to the relatively high activities of NAD-dependent glyceraldehyde 3-phosphate dehydrogenase (NAD-GAPDH, EC 1.2.1.12) and phosphoglycerokinase (PGK, EC 2.7.2.3) which have activities about 500 times higher than GlyK. The two growth conditions had similar enzyme profiles and only two enzymes had significantly different activities ($p < 0.05$ as by Student's t-test; Fig. 1): PEPC is higher by 60% on inorganic nitrogen, while aspartate amino transferase (AspAT, EC 2.6.1.1) exhibits a lower activity on inorganic nitrogen by 37%, (discussed in Section 2.5). Nitrate reductase (NR, EC 1.7.1.1) was measured but almost undetectable, even when nitrate was present in the medium.

There is a good correlation of the enzyme profiles of cultivated embryos with data obtained from former studies, in which *B. napus* developing embryos were taken directly from the intact plant and numerous enzymes of central metabolism were measured (Kang and Rawsthorne, 1994; Eastmond and Rawsthorne, 2000; Hill et al., 2003). For the combined cytosolic and plastidic activities that were reported by Eastmond and Rawsthorne (2000), the following enzymes were measured in this study as well: PGK, NAD-GAPDH, PK and NADP-dependent glyceraldehyde 3-phosphate dehydrogenase (NADP-GAPDH, EC 1.2.1.13). For these four enzymes correlation coefficients were calculated considering all combinations of the two conditions measured in this study and the three developmental stages reported by Eastmond and Rawsthorne (2000): in each case Pearson's correlation coefficient was at least $R = 0.985$ with an probability of error of at maximum $p = 0.015$ (data not shown). Also on an absolute basis (nmol g fw^{-1} min^{-1}), values are very similar between the two studies. This suggests that the metabolic activity (enzyme profile) detected in the cultivated embryos is comparable to that of embryos taken out of developing siliques of intact plants.

2.5. Comparison of enzyme activities and fluxes

When comparing the *in vitro* enzyme activities (Fig. 1) and *in vivo* flux rates (Table 3), there are seven enzymes that can be directly associated with the measured fluxes (Table 3). All of these maximal enzyme activities are higher than the respective net fluxes by factors between 4 and 6700

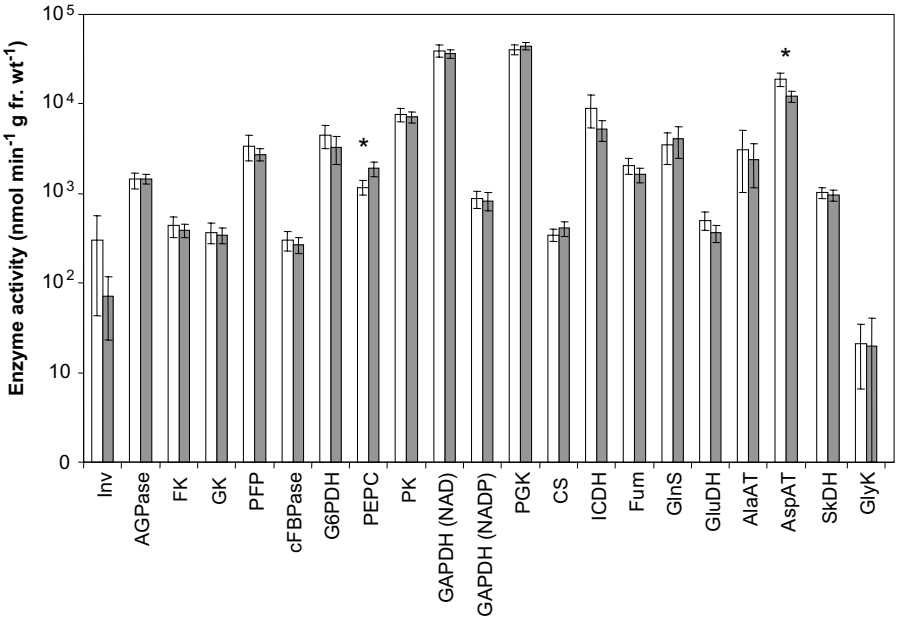

Fig. 1. Enzyme activities measured in rapeseed embryos grown in culture for 12 days with organic (white bars) or inorganic nitrogen sources (grey bars). Enzymes were assayed by robotized metabolite cycling assays. Activities are shown in nmol min^{-1} g fw^{-1} on a logarithmic scale as mean of 10 independent replicates ±95% confidence interval for the mean. Asterisks indicate significant differences between the growth conditions based on a 5% confidence level. Abbreviations: AGPase: ADP-glucose pyrophosphorylase; AlaAT: alanine aminotransferase; AspAT: aspartate aminotransferase; cFBPase: fructose bisphosphatase; CS: citrate synthase; FK: fructokinase; Fum: fumarase; G6PDH: glucose 6-phosphate dehydrogenase; GAPDH (NAD): glyceraldehyde 3-phosphate dehydrogenase; GAPDH (NADP): glyceraldehyde 3-phosphate dehydrogenase; GK: glucokinase; GlnS: Glutamine synthethase; GluDH: Glutamate dehydrogenase; GlyK: glycerol kinase; ICDH: isocitrate dehydrogenase (NADPH); Inv: invertase; NR: nitrate reductase; PEPC: phosphoenolpyruvate carboxylase; PFP: pyrophosphate dependent phosphofructokinase; PGK: phospho-glycerokinase; PK: Pyruvate kinase; SkDH: shikimate dehydrogenase.

times and no correlation can be observed (Fig. 3). This means that the measured enzyme activities are in excess of requirements for the calculated *in vivo* catalytic activities and that in this system measurement of enzyme activity is unlikely to provide meaningful estimates of *in vivo* flux. In addition, between the organic and the inorganic N condition the changes in enzyme activities were often not consistent with changes in measured flux, in particular considering that flux direction for three enzymes shown in Fig. 3 changes. The reversal of the direction of flux between citrate, KG, Glu and Gln (Fig. 2A and B) is not accompanied by changes in the activities of enzymes directly associated to these fluxes indicating that flux is driven by mass balances of other reactions supplying metabolites to or withdrawing metabolites from the network shown in Fig. 2.

Considering an organism as an open system, flux in central metabolism cannot be entirely defined by gene expression. For example, Yang et al. (2002b) grew the cyanobacterium *Synechocystis* under auto-, hetero- and mixotrophic conditions, resulting in big differences in the flux distribution in central metabolism. However, a lack of correlation between transcript levels, protein levels and the change in flux in central metabolism was observed (Yang et al., 2002a). Similar observations were made for yeast grown on different carbon sources (Daran-Lapujade et al., 2004). In both examples, depending on the carbon source used by the organism, the direction of flux may even reverse in parts of central metabolism (glycolysis, citrate cycle) without change in related transcript or protein levels. These examples show that flux in central metabolism can be dictated to a large extent by the prevailing physiological, nutritional and thermodynamic conditions.

A change from the organic to the inorganic nitrogen sources should influence gene expression in the embryos. It has been well established that in leaves, nitrate induces the enzymes NR, PEPC, PK, citrate synthase (CS, EC 2.3.3.1) and NADP-ICDH in a concerted way in order to divert more carbon towards KG and nitrate assimilation (Stitt et al., 2002). Under the inorganic nitrogen condition in this study we could not see this induction pattern. Only PEPC was significantly increased by 60% as compared to the organic nitrogen condition. This increased PEPC activity coincides with an increase in PEPC flux by 31.8 nmol min^{-1} g fw^{-1} (Table 3), which supplies more oxaloacetate (OAA) for the TCA cycle. However, this is not enough to account for the reversal in flux between citrate and KG which accounts for a change of 51.7 nmol min^{-1} g fw^{-1}. A part of the flux adjustment that allows an increased flux between citrate and Glu is achieved by reduction of the malate consumption by NAD-ME which amounts to 19.2 nmol min^{-1} g fw^{-1} (Table 3). Therefore, based on flux analysis presented here, we observe that the enzymes PEPC and NAD-ME allow

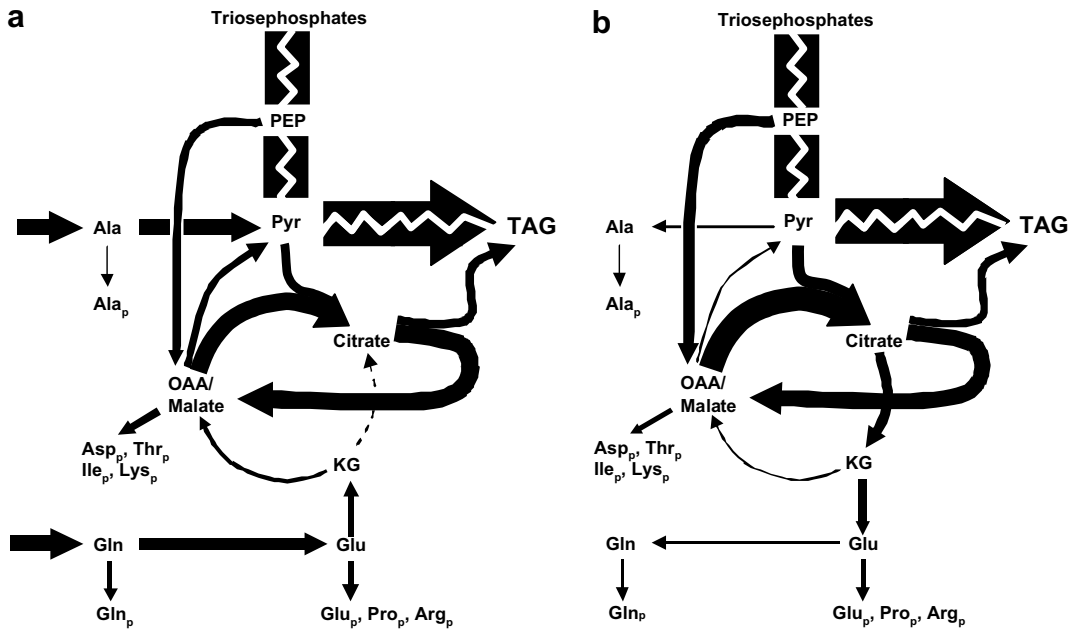

Fig. 2. Visualization of net fluxes related to the citrate cycle in developing *B. napus* embryos, as determined by flux parameter fitting after steady-state labeling: (a) Embryos grown with Gln/Ala as nitrogen source and labeled with a combination of several ^{13}C- and ^{15}N-labeling experiments (flux values taken from Schwender et al., 2006) and (b) Embryos grown with NH_4NO_3 as nitrogen source and labeled with [1-^{13}C]glucose. Flux values, statistics and definition of reactions see Table 3. Arrow thickness is scaled to net flux of carbon, except for fluxes between PEP, Pyr and FAS for which arrow thickness is downsized about 5 times. TAG, triacylglycerol; PEP, phosphoenol pyruvate; pyr, pyruvate; OAA, oxaloacetate; KG, ketoglutarate. The index$_p$ denotes protein-bound amino acids.

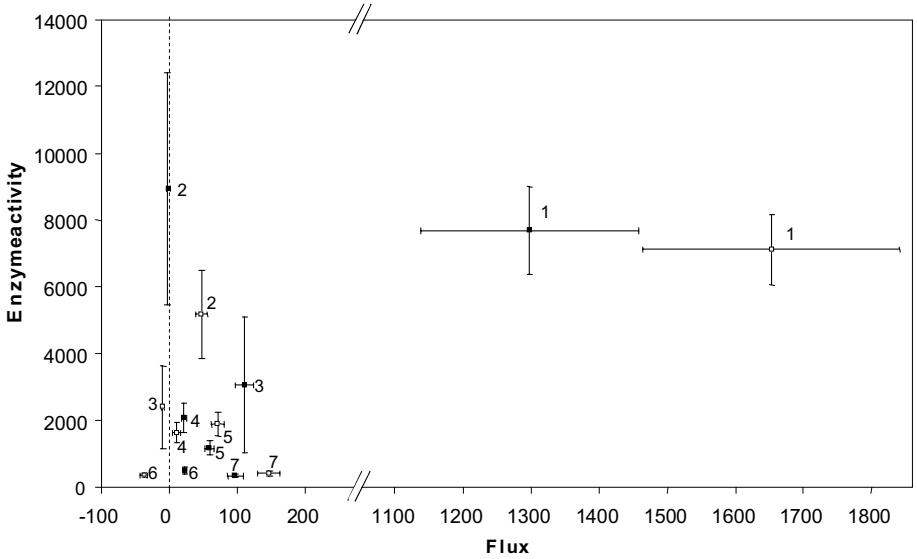

Fig. 3. Comparison of enzyme activities and net fluxes for *B. napus* embryos cultivated under two nutritional conditions. Black squares: organic nitrogen (Gln, Ala); Open squares: inorganic nitrogen (NH_4NO_3). Values are given in nmol min^{-1} g fw^{-1} ±95% confidence interval of the mean. 1: Pyruvate kinase; 2: isocitrate dehydrogenase; 3: alanine aminotransferase; 4: fumarase; 5: phosphoenolpyruvate carboxylase; 6: glutamate dehydrogenase; 7: citrate synthase.

flexible adaptation of flux in response to the changed nutritional condition.

In addition to the observed significant changes in PEPC and AspAT enzyme activities (Fig. 1), the enzymes NADP-ICDH and GluDH decreased significantly based on a 7% significance level. GluDH has been associated with conditions other than primary nitrogen fixation, suggesting a role to replenish TCA-cycle metabolites by converting Glu back to KG under certain conditions (Lancien et al., 2000). Therefore the enzyme could have a role in net conversion of Glu to KG under the Gln/Ala condition while glutamine synthethase (GS, EC 6.3.1.2) and glutamate oxo-

glutarate aminotransferase (GOGAT, EC 1.4.1.14) would be responsible for the reverse net flux observed under the NH_4NO_3 condition (Fig. 2).

As described above, we generally observed higher enzyme activities than fluxes. This is true with one exception. Nitrate reductase activity (NR, EC 1.7.1.1) was present at levels so low (about 30 nmol min^{-1} g fw^{-1}) that the signal could not be reliably detected, even when nitrate was present at 10 mM in the medium. From the observed uptake rates of Ala and Gln under the organic condition (Table 3) one can derive that about 250 nmol nitrogen min^{-1} g fw^{-1} has to be assimilated for the organism to grow at the observed speed. Therefore, under the inorganic nitrogen condition, a maximal flux of 10 nmol min^{-1} g fw^{-1} nitrate reductase can only supply a fraction of the necessary assimilation rate (8% of the nitrogen assimilation rate, if the 50% reduction in growth speed observed under the inorganic nitrogen condition is factored in) and therefore it appears that it is mainly NH_4 that is supporting growth. In accordance with only a marginal ability to assimilate nitrate, developing *B. napus* embryos grow at very much reduced speed on a liquid culture medium with potassium nitrate as sole nitrogen source (data not shown). In addition, nitrate assimilation in *B. napus* plants appears not to take part in pod tissue and remobilized nitrogen to support protein synthesis during seed filling (Rossato et al., 2001).

3. Conclusions

This study demonstrates the plasticity of central metabolism in developing *Brassica napus* embryos in response to changes of nutritional conditions. NH_4NO_3 can be used as a nitrogen source, but nitrate assimilation is obviously not in the range of inducible metabolic responses of developing *B. napus* embryos. Dependent on the nature of the available nitrogen source, metabolic flux is redirected around the TCA cycle in order to sustain the precursor requirements for the biosynthesis of storage compounds. Here metabolic adjustment between organic and inorganic N sources was possible in big parts without major reprogramming of metabolism. However, increase in PEPC activity and increase in PEPC flux indicates the existence of a top-down regulatory response to the presence of inorganic nitrogen sources. While by its anaplerotic function this enzyme may have a pivotal role in carbon partitioning if inorganic nitrogen is used, the carbon flux diverted by the enzyme would not be essential for amino acid synthesis if amino acids related to the TCA cycle (Gln, Glu, Asp, Asn) are used as nitrogen sources (Schwender et al., 2006). Further studies of this kind are intended to identify regulatory principles which are responsible for adaptation of metabolism to change in environmental conditions and which may have control over carbon partitioning as well. In this context the identification of rigid branch points in metabolic networks is possible with our methods described here. Such rigid branch points have been described as a major hurdle to be overcome in metabolic engineering of microorganisms (Stephanopoulos and Vallino, 1991). Studies, such as the one present here, where the response of central metabolism to environmental or genetic perturbation is analyzed at several levels, may help to develop strategies for rational modification of seed composition and plant metabolism in general.

4. Experimental

D-[1-^{13}C]glucose and D-[U-$^{13}C_6$]glucose were purchased from Sigma (St. Louis, MO). Chemicals and enzymes for the enzyme assays were purchased from Roche (Indianapolis, IN) and Sigma.

4.1. Embryo culture

Oilseed rape plants (*Brassica napus* L., cv. Reston) were grown as described before (Schwender and Ohlrogge, 2002). Siliques were harvested 20 days after flowering, and embryos at the early stage of oil accumulation (0.5–1 mg fw) were immediately dissected under aseptic conditions and transferred into a liquid culture medium and cultured for 12 days in 15 ml of growth medium in 250 ml Falcon Tissue Culture Flasks with vented caps (Fisher Scientific, Pittsburgh, PA) under constant temperature and low light conditions (22 °C, continuous light of 50 μmol m^{-2} s^{-1}). Two different liquid growth media were used with inorganic nutrients, microelements and vitamins and polyethylene glycol 4000 (20% w/v) according to Schwender and Ohlrogge (2002) with 80 mM sucrose and 40 mM glucose as the main organic constituents (Schwender et al., 2003). In addition, either Gln and Ala were added (35 and 10 mM, respectively; Schwender et al., 2003) or KNO_3 and NH_4NO_3 were added as sole nitrogen source as described earlier (19 and 10 mM, respectively; Schwender and Ohlrogge, 2002). For ^{13}C-labeling in the ammonium nitrate medium, glucose was replaced with D-[1-^{13}C]glucose or D-[U-$^{13}C_6$]glucose. After culture, embryos were rinsed quickly 3 times in 0.3 M NaCl and immediately snap-frozen in liquid nitrogen. Embryos were stored at −70 °C until analysis.

4.2. Enzyme assays

Most of the activities of the enzymes listed in Fig. 1 were assayed using stopped enzyme assays with subsequent metabolite cycling assays for product quantification as described previously (Gibon et al., 2002, 2004). Nitrate reductase and glutamine synthetase were determined using end point assays and invertase using a stopped assay as described by Gibon et al. (2004).

Frozen embryos were ground to a fine powder and aliquots of a known mass (c. 10 mg fresh weight) of ground embryo tissue were weighed cryogenically. Enzymes were

extracted from these aliquots by vortexing and mixing in 500 μl of common extraction buffer [10% (v/v) glycerol, 0.25% (w/v) BSA, 0.1% (v/v) Triton X-100, 50 mM Hepes/KOH, pH 7.5, 10 mM $MgCl_2$, 1 mM EDTA, 1 mM EGTA, 1 mM benzamidine, 1 mM ε-aminocapronic acid, 1 mM phenylmethylsulfonyl fluoride (PMSF), 10 mM leupeptin, 1 mM dithiothreitol (DTT)] and 10 mg polyvinyl pyrrolidone. PMSF was added just before extraction. DTT was omitted when using peroxidase-based or MTT-based indicator reactions (MTT: methylthiazolyldiphenyl-tetrazolium bromide). A 96-head liquid handling robot (Evolution P3, Perkin Elmer, Wellesey, MA) was used to perform subsequent dilutions of these initial extracts and to plate out and mix the extracts and buffers prior to starting the assays. During this process micro plates were maintained at 4 °C using peltier cooled blocks. Reactions were started with the addition of a given substrate or co-factor as described by Gibon et al. (2004) and incubated at 25 °C for a know time period, usually 15 min. Reactions were then stopped using 0.5 M HCl or 0.5 M NaOH. The concentration of the products of these stopped reactions (NAD^+, NADH, NADPH or glycerol-3-phosphate) was then determined in cycling assays as described by Gibon et al. (2004). Full details of each individual stopped assay and the subsequent cycling assay are described in depth by Gibon et al. (2004) and are not repeated here.

4.3. Analysis of labeling and modeling

After labeling with [1-^{13}C]glucose or [U-$^{13}C_6$]glucose in the NH_4NO_3-medium, embryos were homogenized for 30 s in ice-cold methanol/H_2O (4:3 v/v) using an Omni tissue grinder (Omni Int., GA). After heating to 70 °C for 15 min, $CHCl_3$ was added in order to achieve a mixture of $CHCl_3$:methanol:H_2O = 8:4:3 (v/v) (Folch et al., 1957). After centrifugation the methanol/water phase, the lipid phase and the insoluble residue were separated, solvents removed under a stream of nitrogen and samples dried under vacuum and the fractions analyzed gravimetrically. A part of the insoluble cell residue was further analyzed using a CHNS/O elemental analyzer (Perkin Elmer Series II 2400) configured for CHN analysis. The resulting fractions of lipid and protein (wt/dry wt) determine biomass fluxes as described in Schwender et al. (2006).

Analysis of monomers of lipids, proteins and starch by GC–MS was performed according to Schwender et al. (2003). Lipids were reduced under hydrogen (Pt(IV) oxide catalyst) and the saturated fatty acids were trans-esterified to form methyl esters as described previously (Schwender et al., 2003). After heating the insoluble cell residue in water to 100 °C for 1 h to dissolve starch, the insoluble cell residue was hydrolyzed in 6 N HCl and the amino acids were derivatized to *N*,*O*-*tert*-butyldimethylsilyl (TBDMS) derivatives as described previously (Schwender et al., 2003). Glucose was released from starch by hydrolysis and analyzed as glucose methoxime penta-acetate as described earlier (Schwender et al., 2003). Fatty acid methyl esters and TBDMS-amino acids were analyzed with a gas chromatograph–mass spectrometer (6890N GC/5975 quadrupole MS, Agilent Technologies, Wilmington, DE). The carrier gas was helium at a flow rate of 1 ml/min with a DB1 column (30 m × 0.25 mm; J&W Scientific, Folsom, CA). For saturated fatty acid methyl esters the McLafferty fragment (*m*/*z* 74) was analyzed to determine the fractional labeling in the fragment comprising carbons one and two of each fatty acid (Schwender et al., 2003). In addition to fragment *m*/*z* 74, fragment *m*/*z* 87, representing carbons one, two and three of fatty acids (Murphy, 1993) was analyzed in an analogous way. Considering that odd-numbered carbons in fatty acids are biosynthetically derived from the carboxyl-group of acetyl-CoA, the combination of labeling information from fragments *m*/*z* 74 and *m*/*z* 87 allowed to determine the ^{13}C-enrichment in C-1 of fatty acids according to probabilistic equations. For each GC–MS chromatogram of amino acid derivatives 136 mass isotopomer fractions were recorded, whereas for fatty acid methyl esters, glycerol and glucose derivatives 29 mass isotopomer fractions were monitored. In general, the relative abundances of mass isotopomers in selected fragments of each analyzed derivative were measured using selected ion monitoring. Correction for the occurrence of ^{13}C in derivative parts of the molecules and for heavy isotopes in heteroatoms (C, H, O, N, and Si) at their natural abundances was performed as described earlier (Schwender et al., 2003). Finally MS measurements from analysis of embryos grown in three separate vessels were averaged.

Central metabolism of developing *B. napus* embryos grown on NH_4NO_3-medium was modeled including reactions of glycolysis, oxidative pentose phosphate pathway, ribulose 1,5-bisphosphate carboxylase/oxygenase and tricarboxylic acid cycle as described in detail earlier (Schwender et al., 2006). This includes implementation of details of the network topology established earlier by analyzing a series of different labeling experiments under the Gln/Ala growth condition (Schwender et al., 2006). Accordingly the following assumptions are assigned to the model used for flux analysis of the NH_4NO_3 condition: (1) Asp represents label in oxaloacetate, malate and fumarate, as these pools are interconverted very fast resulting in isotopic equilibration. This assumption for the NH_4NO_3 condition is supported by the consistently high fumarase activity under both conditions (Fig. 1). (2) Reversibility of interconversion of α-ketoglutarate and citrate (Aconitase, isocitrate dehydrogenase). (3) Cytosolic acetyl-CoA is formed from citrate by ATP:citrate lyase (ACL, EC 2.3.3.8) and accordingly label in the terminal acetate units of C_{20} and C_{22} fatty acids represents carbons C-2 + C-3 of mitochondrial pyruvate. (4) High aminotransferase activities equilibrate label in pyruvate, α-ketoglutarate, oxaloacetate with Ala, Asp and Glu, respectively. The consistently high activities of Ala- and Asp aminotransferase under both conditions (Fig. 1) clearly support this assumption. (5) Non-presence of the glyoxylate cycle. Without the

influx of Ala and Gln from the in the NH_4NO_3-medium, flux between cytosolic and plastidic pools of pyruvate could not be resolved as described before (Schwender et al., 2006). However, this does not impact the conclusions drawn in this study.

Flux parameter fitting and statistical analysis were performed using the software package *13CFLUX* obtained from Dr. W. Wiechert (Department of Simulation, University of Siegen, Germany; Wiechert et al., 2001) including the Sequential Quadratic Programming algorithm by Peter Spellucci (Technical University Darmstadt, Germany) as described before (Schwender et al., 2006). For labeling with [1-^{13}C]glucose the measured mass spectrometric ^{13}C-labeling patterns in 15 fragments of 8 selected metabolites were used for flux parameter fitting: (a) Asp, (b) Pro, (c) Ala (d) glucose (starch hydrolysis) and the terminal acetate units of (e) C18 and (f) C22 fatty acids, representing the metabolite pools of (a) oxaloacetate, (b) α-ketoglutarate, (c) pyruvate, (d) hexose phosphates, (e) plastidic and (f) cytosolic acetyl-CoA, respectively (Table 2). In addition, from labeling with [U-$^{13}C_6$]glucose 7 fragments from Asp, Pro and Ala were considered for flux parameter fitting (Table 2). By varying the values for six freely variable net fluxes in the system a best fit between predicted and measured mass isotopomer abundances was obtained by minimizing the sum of squared differences. Flux parameter fitting was started more than 50 times with randomly chosen starting values for the free flux parameters (randomly chosen within the feasible flux space) and one best fit was consistently obtained.

Acknowledgements

This work was supported by the Office of Basic Energy Sciences (J.S.) and, in part, by the Office of Biological and Environmental Research, Program for Ecosystem Research (AR) of the US Department of Energy. We thank Dr. Yves Gibon for instruction in the analysis of enzyme activities.

References

Daran-Lapujade, P., Jansen, M.L., Daran, J.M., van Gulik, W., de Winde, J.H., Pronk, J.T., 2004. Role of transcriptional regulation in controlling fluxes in central carbon metabolism of *Saccharomyces cerevisiae*. A chemostat culture study. J. Biol. Chem. 279, 9125–9138.

Eastmond, P.J., Rawsthorne, S., 2000. Coordinate changes in carbon partitioning and plastidial metabolism during the development of oilseed rape embryo. Plant Physiol. 122, 767–774.

Fell, D.A., 1997. Understanding the Control of Metabolism. Portland Press.

Folch, J., Lees, M., Sloane-Stanley, G.H.S., 1957. A simple method for the isolation and purification of total lipids from animal tissues. J. Biol. Chem. 226, 497–509.

Gibon, Y., Vigeolas, H., Tiessen, A., Geigenberger, P., Stitt, M., 2002. Sensitive and high throughput metabolite assays for inorganic pyrophosphate, ADPGlc, nucleotide phosphates, and glycolytic intermediates based on a novel enzymic cycling system. Plant J. 30, 221–235.

Gibon, Y., Blaesing, O.E., Hannemann, J., Carillo, P., Höhne, M., Hendriks, J.H.M., Palacios, N., Cross, J., Selbig, J., Stitt, M., 2004. A robot-based platform to measure multiple enzyme activities in *Arabidopsis* using a set of cycling assays: comparison of changes of enzyme activities and transcript levels during diurnal cycles and in prolonged darkness. Plant Cell 16, 3304–3325.

Goffman, F.D., Alonso, A.P., Schwender, J., Ohlrogge, J.B., Shachar-Hill, Y., 2005. Light enables a very high efficiency of carbon storage in developing embryos of rapeseed. Plant Physiol. 138, 2269–2279.

Heinrich, R., Rapoport, T.A., 1974. A linear steady-state treatment of enzymatic chains. Eur. J. Biochem. 42, 89–95.

Hill, L.M., Morley-Smith, E.R., Rawsthorne, S., 2003. Metabolism of sugars in the endosperm of developing seeds of oilseed rape. Plant Physiol. 131, 228–236.

Hirai, M.Y., Yano, M., Goodenowe, D.B., Kanaya, S., Kimura, T., Awazuhara, M., Arita, M., Fujiwara, T., Saito, K., 2004. Integration of transcriptomics and metabolomics for understanding of global responses to nutritional stresses in *Arabidopsis thaliana*. Proc. Natl. Acad. Sci. USA 101, 10205–10210.

Hirai, M.Y., Klein, M., Fujikawa, Y., Yano, M., Goodenowe, D.B., Yamazaki, Y., Kanaya, S., Nakamura, Y., Kitayama, M., Suzuki, H., Sakurai, N., Shibata, D., Tokuhisa, J., Reichelt, M., Gershenzon, J., Papenbrock, J., Saito, K., 2005. Elucidation of gene-to-gene and metabolite-to-gene networks in *Arabidopsis* by integration of metabolomics and transcriptomics. J. Biol. Chem. 280, 25590–25595.

Kacser, H., Burns, J.A., 1973. The control of flux. Symp. Soc. Exp. Biol. 27, 65–104.

Kang, F., Rawsthorne, S., 1994. Starch and fatty-acid synthesis in plastids from developing embryos of oilseed rape (*Brassica napus*). Plant J. 6, 795–805.

Lancien, M., Gadal, P., Hodges, M., 2000. Enzyme redundancy and the importance of 2-oxoglutarate in higher plant ammonium assimilation. Plant Physiol. 123, 817–824.

Li, R.J., Wang, H.Z., Mao, H., Lu, Y.T., Hua, W., 2006. Identification of differentially expressed genes in seeds of two near-isogenic *Brassica napus* lines with different oil content. Planta 224, 952–962.

Morcuende, R., Bari, R., Gibon, Y., Zheng, W., Pant, B.D., Blasing, O., Usadel, B., Czechowski, T., Udvardi, M.K., Stitt, M., Scheible, W.R., 2007. Genome-wide reprogramming of metabolism and regulatory networks of *Arabidopsis* in response to phosphorus. Plant Cell Environ. 30, 85–112.

Murphy, C.M., 1993. Mass spectrometry of lipids. In: Snyder, F. (Ed.), . In: Handbook of Lipid Research, vol. 7. Plenum Press, New York, pp. 71–130.

Petersen, S., Mack, C., de Graaf, A.A., Riedel, C., Eikmanns, B.J., Sahm, H., 2001. Metabolic consequences of altered phosphoenolpyruvate carboxykinase activity in *Corynebacterium glutamicum* reveal anaplerotic regulation mechanisms *in vivo*. Metabol. Eng. 3, 344–361.

Roessner, U., Luedemann, A., Brust, D., Fiehn, O., Linke, T., Willmitzer, L., Fernie, A.R., 2001. Metabolic profiling allows comprehensive phenotyping of genetically or environmentally modified plant systems. Plant Cell 13, 11–29.

Rontein, D., Dieuaide-Noubhani, M., Dufourc, E.J., Raymond, P., Rolin, D., 2002. The metabolic architecture of plant cells. Stability of central carbon metabolism and flexibility of anabolic pathways during the growth cycle of tomato cells. J. Biol. Chem. 46, 43948–43960.

Rossato, L., Laine, P., Ourry, A., 2001. Nitrogen storage and remobilization in *Brassica napus* L. during the growth cycle: nitrogen fluxes within the plant and changes in soluble protein patterns. J. Exp. Bot. 52, 1655–1663.

Ruuska, S.A., Girke, T., Benning, C., Ohlrogge, J.B., 2002. Contrapuntal networks of gene expression during *Arabidopsis* seed filling. Plant Cell 14, 1191–1206.

Ruuska, S.A., Schwender, J., Ohlrogge, J.B., 2004. The capacity of green oilseeds to utilize photosynthesis to drive biosynthetic processes. Plant Physiol. 136, 2700–2709.

Scheible, W.R., Morcuende, R., Czechowski, T., Fritz, C., Osuna, D., Palacios-Rojas, N., Schindelasch, D., Thimm, O., Udvardi, M.K., Stitt, M., 2004. Genome-wide reprogramming of primary and secondary metabolism, protein synthesis, cellular growth processes, and the regulatory infrastructure of *Arabidopsis* in response to nitrogen. Plant Physiol. 136, 2483–2499.

Schwender, J., Ohlrogge, J.B., 2002. Probing *in vivo* metabolism by stable isotope labeling of storage lipids and proteins in developing *Brassica napus*embryos. Plant Physiol. 130, 347–361.

Schwender, J., Ohlrogge, J.B., Shachar-Hill, Y., 2003. A flux model of glycolysis and the oxidative pentosephosphate pathway in developing *Brassica napus* embryos. J. Biol. Chem. 278, 29442–29453.

Schwender, J., Goffman, F., Ohlrogge, J.B., Shachar-Hill, Y., 2004. Rubisco without the Calvin cycle improves the carbon efficiency of developing green seeds. Nature 432, 779–782.

Schwender, J., Shachar-Hill, Y., Ohlrogge, J.B., 2006. Mitochondrial metabolism in developing embryos of *Brassica napus*. J. Biol. Chem. 281, 34040–34047.

Stephanopoulos, G., Vallino, J.J., 1991. Network rigidity and metabolic engineering in metabolite overproduction. Science 252, 1675–1681.

Stitt, M., Muller, C., Matt, P., Gibon, Y., Carillo, P., Morcuende, R., Scheible, W.R., Krapp, A., 2002. Steps towards an integrated view of nitrogen metabolism. J. Exp. Bot. 53, 959–970.

The Arabidopsis Genome Initiative, 2000. Analysis of the genome sequence of the flowering plant *Arabidopsis thaliana*. Nature 408, 796–815.

Tohge, T., Nishiyama, Y., Hirai, M.Y., Yano, M., Nakajima, J., Awazuhara, M., Inoue, E., Takahashi, H., Goodenowe, D.B., Kitayama, M., Noji, M., Yamazaki, M., Saito, K., 2005. Functional genomics by integrated analysis of metabolome and transcriptome of *Arabidopsis* plants over-expressing an MYB transcription factor. Plant J. 42, 218–235.

Urbanczyk-Wochniak, E., Luedemann, A., Kopka, J., Selbig, J., Roessner-Tunali, U., Willmitzer, L., Fernie, A.R., 2003. Parallel analysis of transcript and metabolic profiles: a new approach in systems biology. EMBO Rep. 4, 989–993.

Wiechert, W., Mollney, M., Petersen, S., de Graaf, A.A., 2001. A universal framework for ^{13}C metabolic flux analysis. Metab. Eng. 3, 265–283.

Yang, C., Huaw, Q., Shimizu, K., 2002a. Metabolic flux analysis in *Synechocystis* using isotope distribution from ^{13}C-labeled glucose. Metab. Eng. 4, 202–216.

Yang, C., Hua, Q., Shimizu, K., 2002b. Integration of the information from gene expression and metabolic fluxes for the analysis of the regulatory mechanisms in *Synechocystis*. Appl. Microbiol. Biotechnol. 58, 813–822.